#1

INVITED REVIEW
Advances in Imaging of Vertebral and Spinal Cord Injury

Andrew L. Goldberg, MD; Sharif M. Kershah, MD

MetroHealth Medical Center, Case Western Reserve University School of Medicine, Cleveland, Ohio

Received August 10, 2009; accepted December 16, 2009

Abstract

Background/Objectives: Imaging technology is an important part of the diagnosis and management of spinal trauma. Indications and findings in post-traumatic imaging of the vertebral column and spinal cord are reviewed.

Methods: An extensive literature review was performed on the imaging of vertebral and spinal cord injury. Relevant images from a Level I trauma center were included as examples.

Results: Imaging plays an important role in the evaluation of acute and chronic spinal injury. Spinal cord and soft-tissue injuries are best evaluated by magnetic resonance imaging (MRI), whereas spinal fractures are better characterized by computed tomography (CT). Vascular injuries can be evaluated using CT or MR angiography.

Conclusions: Imaging using CT and MRI is essential in the management of spinal cord injuries, both in the acute and in the chronic settings. MRI shows the status of ligamentous integrity and visualizes internal derangement of the spinal cord. Vascular compromise can be diagnosed by MR and CT angiography. Plain radiography now has a more limited, adjunctive role, and the need for higher risk myelography has been minimized.

J Spinal Cord Med. Apr 2010;33(2):105–116

Key Words: Spinal trauma; Imaging techniques; Magnetic resonance imaging, angiography, spectroscopy, functional; Computed tomography; Plain radiography; Angiography; Fracture; Spinal cord injuries; Diffusion-weighted imaging; Diffusion tensor imaging

INTRODUCTION

The past several decades have witnessed the rapid development of imaging technology that has dramatically transformed the diagnosis and management of vertebral injury and spinal cord injury (SCI). The advent of magnetic resonance imaging (MRI) has enabled the noninvasive visualization of the spinal cord in a manner previously unimaginable in the living person. An extensive spectrum of both acute and chronic SCI has been demonstrated and has been shown to have prognostic significance. The initial value of MRI in the detection and evaluation of fractures was thought to be limited, but with advances in knowledge and technique, it is now known to be considerable. Concurrently, computed tomography (CT) has also been further perfected and has supplanted plain radiography as the first-line modality for evaluating the traumatized vertebral column.

Please address correspondence to Andrew L. Goldberg, MD, 2500 MetroHealth Drive, Cleveland, Ohio 44109; p: 216 778 4010; f: 216 778 4046 (e-mail: agoldberg@metrohealth.org).

Anatomy Review

A review of normal anatomy is relevant as a basis for understanding pathologic alteration (1) (Figure 1a through d). The spinal axis consists of 7 cervical, 12 thoracic, and 5 lumbar vertebrae, although minor anomalies of segmentation are common. The anatomy of the craniocervical junction has several unique features. C1 (atlas) has no body and articulates with the occipital condyles superiorly. C2 (axis) has a body and a dens or odontoid process that articulates with the anterior arch of C1. This articulation is stabilized by the transverse ligament, which spans the posterior aspect of the dens and attaches to the lateral masses of C1. There is a superior crus of the transverse ligament, which attaches to the clivus, and an inferior crus connects to the C2 body. The alar ligaments run from the tip of the dens to the occipital condyles.

Caudally, from C3 through the thoracolumbar region, the vertebrae are composed of a body, bilateral pedicles, laminae, and articulating facets (both superior and inferior). The spinal cord lies within the bony vertebral canal and is covered by the meninges (pia, arachnoid, and dura). In the mature spinal canal, the termination of the cord (conus medullaris) typically is found at or slightly below the thoracolumbar junction.

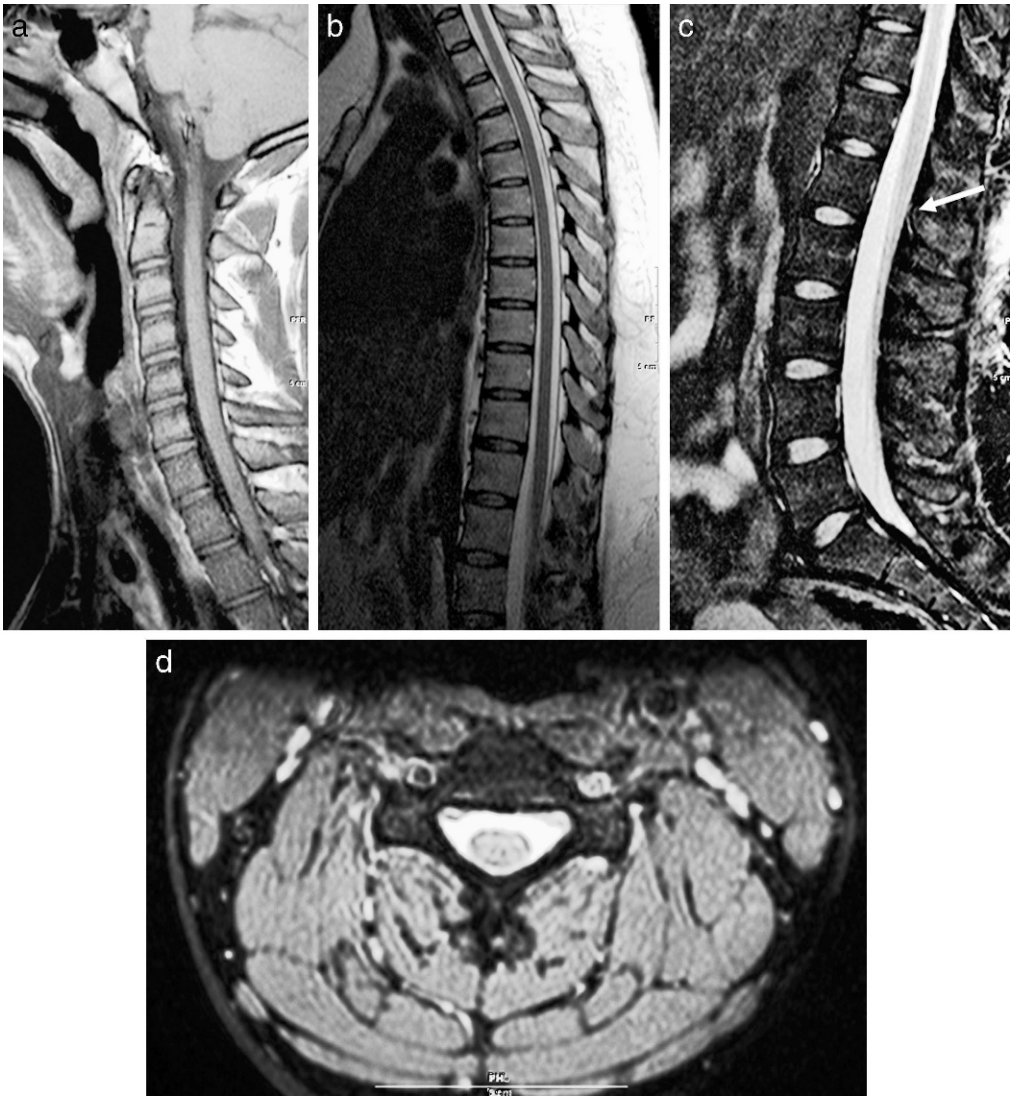

Figure 1. *Normal anatomy. (a) Sagittal T1-weighted image of the cervical spine. (b) Sagittal T2-weighted image of the cervical spine. (c) Sagittal T2-weighted image of the lumbar spine. Notice the normal termination of the spinal cord at the thoracolumbar junction (arrow). (d) Axial T2-weighted image of the cervical spine.*

Paired spinal nerves exit the neural foramina, enclosed by nerve root sheaths, which can occasionally vary in their size and configuration. The intervertebral disks are notochordal remnants that are composed of a tough annulus fibrosus and a more jelly-like central nucleus pulposus. The spine is further stabilized by the anterior and posterior longitudinal ligaments, which adhere to the anterior and posterior aspects of the vertebral bodies, respectively. At their most cephalad extent, these ligaments attach to the basiocciput; the tectorial membrane is an intervening structure between the bone and the posterior longitudinal ligament. The ligamentum flavum provides a continuous connection between the laminae, as the interspinous ligament does for the spinous processes. The ligamentum nuchae (or supraspinous ligament) connects the tips of the spinous processes. The vertebral arteries are enclosed by the foramina transversaria between C2 and C7.

Technical Considerations

Over the past decade, and especially during the last several years, the use of CT for spine trauma screening has become universal, and plain radiography has been virtually relegated to the past (2–4). In one series, of 116 injuries requiring treatment, only 75 were seen on radiography; the remainder was detected by CT (5).

This development has been facilitated by technical advances in multidetector CT, in which the accumulation of submillimeter section data is achieved by helical rotation of the gantry (2,4). This process has become more rapid as scanner design has incorporated an ever larger number of detector arrays, from 16 to 64 and even as high as 256. Images can be reconstructed in a variety of planes at desired section thicknesses (utilizing postprocessing algorithms that can enhance the diagnosis of bony or soft-tissue abnormalities) and can be further modified to display vascular structures (CT angiography) (6).

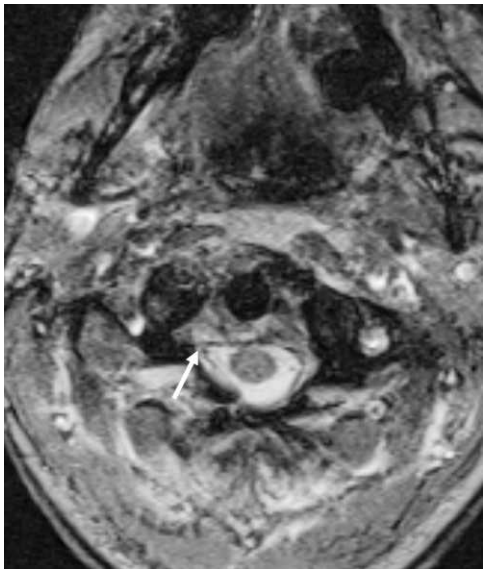

Figure 2. *Causes of spinal stenosis and cord compression. Axial T2-weighted image demonstrating a small epidural hematoma (arrow).*

In the setting of spinal trauma, axial data acquisition followed by sagittal multiplanar reconstruction is the mainstay of initial diagnosis. Coronal reconstructions are also quite useful for visualization of the craniocervical junction, as well as for the remainder of the spinal axis if scoliosis is present. If cervical fractures are detected, most protocols will proceed to CT angiography to exclude vascular (especially vertebral artery) injury (6,7). This technique is even more essential in the setting of penetrating trauma.

Figure 3. *Causes of spinal stenosis and cord compression. Sagittal T2-weighted image demonstrates a disk bulge at C5–C6 (arrow).*

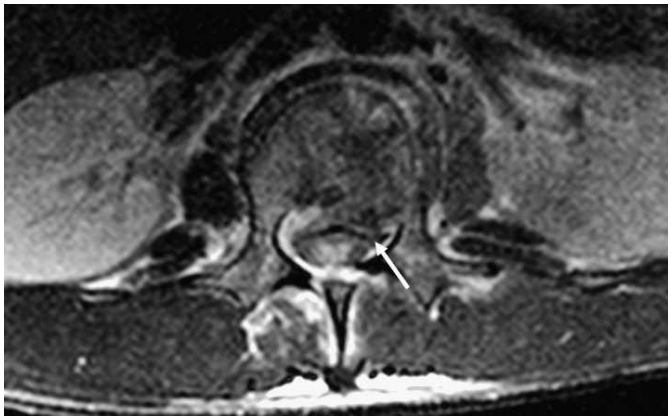

Figure 4. *Causes of spinal stenosis and cord compression. Axial T2-weighted image showing a burst fracture with retropulsion of fragments into the canal (arrow).*

MRI requires much of the sophisticated computing power of CT but is based on very different physical principles. Whereas CT, like plain radiography, detects differences in radiographic attenuation of tissues, MRI exploits the varying relaxivity of hydrogen atoms in response both to the presence of a powerful static magnetic field and to the superimposed time-varying gradient magnetic fields. A detailed discussion of these physical phenomena is beyond the scope of this article (many excellent review articles are available in the literature) (8–10). However, it is important to know that scanning sequence parameters are altered to generate T1- and T2-weighted images. T1-weighted images enhance the signals of fat, proteinaceous fluid, subacute hemorrhage, and intravascular contrast agents. Both bulk phase and edema fluid, by comparison, are hyperintense on T2-weighted images. A similar signal pattern is achieved by short inversion recovery (STIR) imaging, which is a technique that suppresses fat. Additional

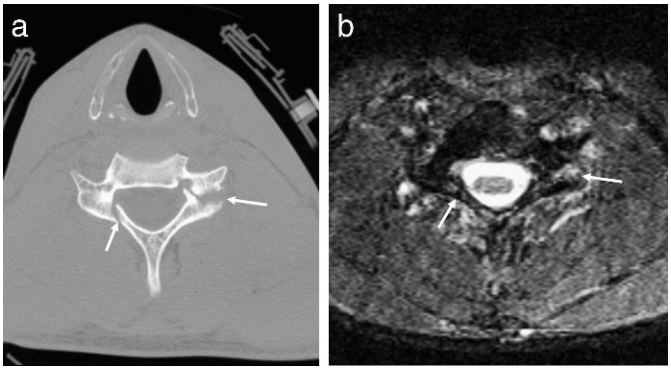

Figure 5. *Bony detail with CT. (a) Axial CT demonstrates fractures of the posterior elements of C5 (arrows). (b) Axial STIR sequence at the same level does not show the fractures as clearly, although soft-tissue and intraosseous edema is present (arrows).*

Figure 6. *Spondylosis and cord injury. Sagittal T2-weighted image with increased signal within the spinal cord at the C6 level consistent with contusion (arrow). No fracture or ligamentous injury was identified.*

Figure 7. *Cord contusion. T2-weighted image demonstrates a compression fracture of C5 causing cord edema and swelling (arrow).*

techniques that highlight the presence of hemorrhage by increasing the conspicuity of signal loss include gradient echo imaging and, more recently, susceptibility-weighted imaging. Administration of intravenous contrast (gadolinium chelate) is generally not necessary to evaluate the traumatized vertebral column.

Diffusion-weighted imaging (DWI) employs especially rapid echo planar sequences that interrogate changes in the random motion of water protons. This technique is well established in cerebral ischemia and in traumatic brain injury. Evaluation of the spinal cord is more difficult with DWI due to the relatively small region of interest, cardiorespiratory motion, and cerebrospinal fluid (CSF) pulsations, but recent work has demonstrated potential utility in further assessing SCI (11,12).

Safety should always be borne in mind before MRI is performed, especially in the setting of acute spinal injury (13–17). It must always be recognized that the main magnetic field is 100,000 times more powerful than the ambient terrestrial magnetic field. Foreign objects brought into the scanner room must be MRI compatible. Cardiac pacemakers, neurostimulator devices, cochlear implants, and coiled wires should be avoided. Implanted orthopedic devices, inferior vena cava filters, and intravascular stents are generally safe at 1.5 Tesla. Hemodynamic monitoring is important; electrocardiographic tracings may be somewhat inconsistent, but blood pressure and pulse oximetry measurements are generally reliable. The patient should be stabilized on a slider board to minimize neck movement. Finally, direct video observation of the patient should be performed.

SPECTRUM OF INJURY

MRI is capable of providing exquisite detail regarding the appearance of the spinal cord after injury. Such injuries can be subdivided into those that relate to extrinsic compression and those that traumatize the cord parenchyma itself.

Fractures with bony retropulsion, disk extrusions, and epidural hematomas can result in cord compression, often concomitantly (Figures 2 through 4). MRI will generally be successful, based on characteristic morphologic and signal criteria, in differentiating these compressive abnormalities (18). CT is a useful adjunct, certainly, in delineating bony detail (Figure 5a and b) and is important in preoperative planning (4,19,20). Preexisting spondylosis and spinal stenosis will accentuate the vulnerability of the cord to extrinsic compression (Figure 6), and the severity of cord compression has an

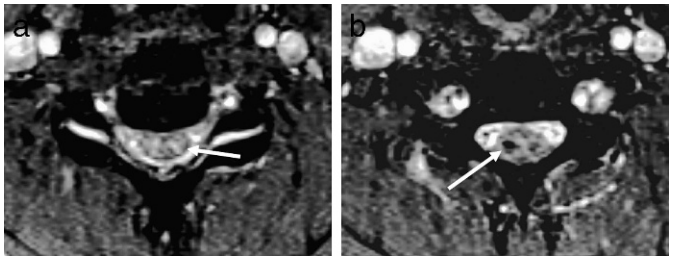

Figure 8. *Cord contusion and hemorrhage. (a) Axial T2-weighted image in a different patient showing increased signal consistent with cord contusion (arrow). (b) Additional T2-weighted image images more inferiorly show signal dropout consistent with areas of cord hemorrhage (arrow).*

adverse correlation with prognosis, independent from intrinsic cord injury (21–23).

The spectrum of acute SCI includes (a) swelling, defined as a smooth enlargement of the cord contour; (b) edema, where internal signal demonstrates T1 and T2 prolongation (low and high signals, respectively) (Figures 7 and 8a); and (c) hemorrhage, where the signal alteration is somewhat complex and evolves temporally (Figure 8b). Most reliably, acute intramedullary hemorrhage is seen as a focus of T2 shortening (hypointensity) (24). Cervical cord hematomas have a strong correlation with a complete neurologic deficit: ASIA A, with the highest lesions carrying an increased risk of fatality (especially at the cervico-medullary junction in the setting of occipito-atlantal dislocation) (23,25). At any level, the cord is vulnerable to transection if the applied forces are sufficient. It should be noted, however, that a presumption of cord transection cannot be made, even with a severe fracture dislocation evident on CT.

In the subacute to chronic time period, additional aspects of cord injury can become apparent. Myelomalacia demonstrates signal alteration equivalent to edema, that is, T2 hyperintensity and T1 signal intermediate between cord and CSF (26). Associated cord swelling tends to diminish compared with edema seen in the acute setting; however, in the early subacute period, a recent article has shown that the cephalo-caudal extent of cord edema can increase by an average of one full vertebral body level if imaging is performed 48 to 72 hours after injury, rather than within the first 24 hours (25).

In recent years, an additional entity, progressive post-traumatic myelomalacic myelopathy (PTMM), has been recognized (27,28) and is most relevant in the late subacute period (generally more than 2 months post injury). The etiology of this injury is not fully understood, but it likely represents a presyrinx state following disruption of normal transparenchymal CSF transit. A contributory role for cord tethering by adhesions has also been proposed, which may be amenable to intraoperative lysis (28,29). Typically, the progressive lesion ascends (often over a long segment) or descends from the site of original trauma. Figure 9 a through d demonstrates a case in which the new myelomalacic abnormality was cephalad to but noncontiguous with the initial injury.

In certain cases, long after the initial injury, a chronic post-traumatic cord cyst or syrinx will develop. These can be identified as expansile structures that are isointense

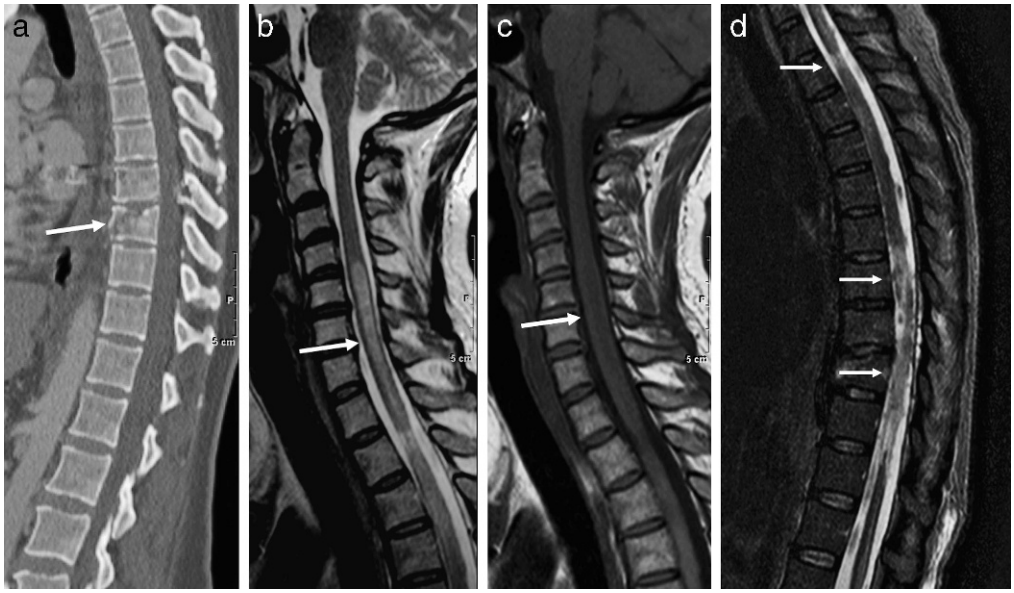

Figure 9. *PPMM. (a) Sagittal CT demonstrates a gunshot wound through the spinal canal at the T8–T9 level (arrow). (b) Sagittal T2-weighted image a few months later demonstrates abnormal signal (arrow) much higher in the cord compared with the primary injury. (c) On the sagittal T1-weighted image, the lesion is slightly hypointense to the cord (arrow). Note that the signal intensity of the lesion is more consistent with edema than cyst formation. (d) The sagittal STIR demonstrates cord signal abnormality at the level of the injury extending cranially (arrows).*

Figure 10. *Syrinx. Sagittal T2-weighted image shows a small syrinx at the C6 and C7 levels following minor trauma (arrow).*

Figure 11. *Syrinx. Sagittal T2-weighted image in a different patient shows extensive syrinx formation throughout the entire cervical cord (asterisks). The abnormality was also isointense to cerebrospinal fluid on T1-weighted image (not shown).*

with CSF on all sequences (26) (Figures 10 and 11) and that are more sharply marginated compared with myelomalacia (30). Some cases of PPMM will evolve into syrinxes (28). Finally, cord atrophy is a well-recognized long-term sequel to SCI and is the most common finding in patients imaged more than 20 years after the initial trauma. Atrophy has been defined as an anterior-posterior (A-P) dimension of 7 mm or less in the cervical cord and 6 mm or less in the thoracic region (29).

Fracture Patterns and Ligamentous Disruption

Forces exerted on the vertebral column that can result in fracture include axial loading, hyperflexion, hyperextension, distraction, and rotational stress. A detailed analysis of spinal biomechanics is beyond the scope of this article, but it is important to identify certain patterns of injury that are evident on radiologic examinations, including plain radiography, CT, and MRI. Although MRI may be more valuable in evaluating soft-tissue structures, CT is superior for the characterization of fractures (18). Preexisting conditions, such as ankylosing spondylitis and diffuse idiopathic skeletal hyperostosis (Figure 12), increase the rigidity of the spine and the risk of fracture (31). Full evaluation of the entire spine should be considered after identification of a fracture, because there is an estimated 16% incidence of noncontiguous spine fractures (32).

Axial loading generates a compressive force that creates a vertebral ''burst fracture'' (33). Typically, a sagittally oriented fracture line through the vertebral body is seen on axial CT images that are associated with a retropulsed fragment (Figure 13a and b). The fracture line may also propagate through the neural arch posteriorly. At C1, this same force can result in a Jefferson

Figure 12. *Sagittal CT demonstrates markedly displaced fracture in a patient with preexisting diffuse idiopathic skeletal hyperostosis.*

fracture, where the anterior and posterior arches are disrupted (Figure 14a and b).

Hyperflexion also typically results in vertebral compression, often associated with anterolisthesis and facet perching or locking (Figure 15a and b). Particularly in the cervical region, a flexion teardrop fracture can occur (34) (Figure 16a and b). These are typically larger fragments than extension teardrop fractures, which occur at the anterior-inferior corner of the vertebral body (31). In the thoracolumbar spine, the Chance or Chance-equivalent fracture is another common manifestation of a flexion injury (35). In such cases, a compression deformity of the vertebral body is associated with a horizontally oriented fracture that propagates through the pedicles and supporting ligaments (Figure 17a and b). In the lower lumbar region, preexisting defects in the pars interarticularis (spondylolysis) are commonly seen and should not be mistaken for acute fractures (Figure 18a through c).

Characteristics of hyperextension injuries include widening of the anterior disk space, retrolisthesis, and

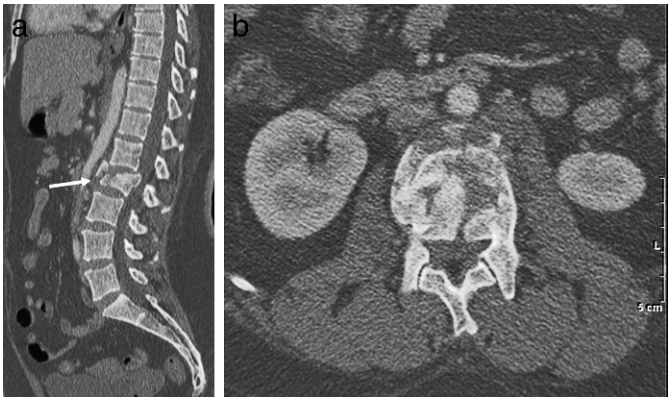

Figure 13. *Burst fracture. (a) Sagittal CT demonstrates a burst fracture of the L2 vertebral body (arrow) with retropulsion of fracture fragments into the spinal canal. (b) Axial CT at the level of the burst fracture.*

neural arch fractures, but without facet dislocation (31) (Figures 19a and b and 20). Distraction injuries can occur in conjunction with rotation as well as other mechanisms, although ligamentous injury, particularly in children, can occur from a distraction mechanism alone (36,37). In such cases, axial images can be deceptively normal; the sagittal and coronal reconstructions are essential to demonstrate the magnitude of disk-vertebral and facet disruption (Figure 21a through c).

As previously reviewed, important ligamentous structures of the vertebral column include the anterior and posterior longitudinal ligaments, interspinous and supraspinous ligaments, and ligamentum flavum. Although injury to these structures can be inferred on CT, they are best visualized on MRI as continuous bands of hypointense signal. Ligamentous tears result in abrupt discontinuity, or if the tear is partial, the injury may be best seen as a focus of ill-defined soft-tissue hyperintensity on T2-weighted or STIR sequences (Figures 22 and 23) (36).

Vascular Compromise

Relevant information can also be gleaned from observing the major arterial structures in the neck, even on standard MR sequences. Both T1- and T2-weighted images should demonstrate flow void in the carotid and vertebral arteries, although this phenomenon can be confounded by flow-related artifacts, especially on T1-weighted sequences (38,39). However, with the application of fat suppression to a T1-weighted axial sequence, an intramural hematoma can be detected in cases of nonocclusive dissection (40–42) (Figures 24a and 25a).

MR angiography can carry the analysis forward by visualizing hyperintense signal in the arteries, which are reconstructed into their anatomically recognizable morphology by maximum intensity projection algorithms (Figure 24b). Artifactual flow gaps, which are occasion-

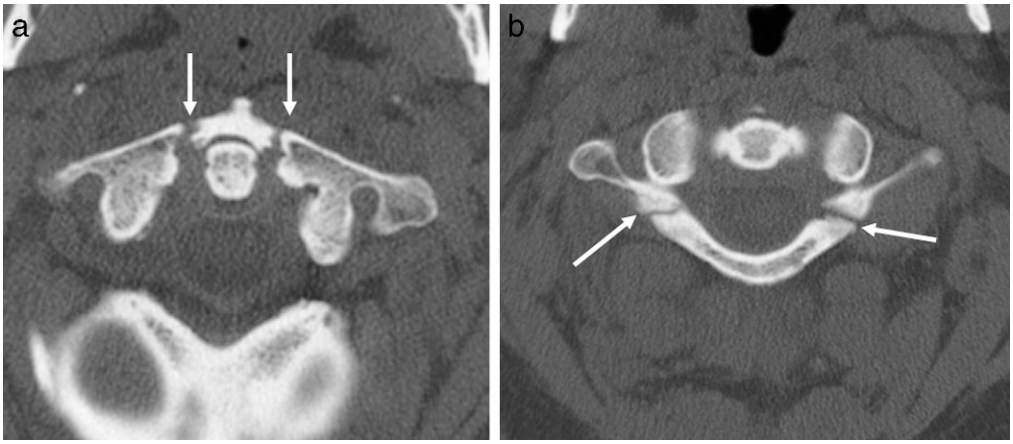

Figure 14. *Jefferson fracture. (a) Axial CT showing bilateral fractures of the anterior arches of C1 (arrows). (b) Axial CT showing bilateral fractures of the posterior arches of C1 (arrows).*

ally problematic, can generally be eliminated if rapid-acquisition, contrast-enhanced sequences are employed (39). Because of the risk of nephrogenic systemic fibrosis, a relatively recently elucidated complication of gadolinium chelates in patients with renal insufficiency (15,17), contrast-enhanced MR angiography is being utilized less often.

CT angiography, in comparison, has been shown to effectively demonstrate carotid and vertebral injury (Figure 25b) and in many institutions has become part of the standard imaging protocol if a cervical vertebral fracture has been documented by noncontrast CT (6,7). There is evidence that CT angiography may be preferable to MR angiography for evaluation of the vertebral arteries in a trauma setting. (43). However, the arterial visualization can be limited if the timing of the contrast bolus is suboptimal, and overlapping bony architecture can also be problematic. In general, with technical expertise and advances in image postprocessing, most practitioners are finding this modality quite useful. Detectable abnormalities include dissection, vascular occlusion, pseudoaneurysm formation, and free-contrast extravasation from an uncontained rupture (6,44) (Figure 18). Differentiating minimal irregularity representing grade I dissection from artifact can be difficult, but this has lesser clinical import compared with the more severe injuries.

New Directions

Relatively new techniques that have shown potential utility in improving the diagnostic assessment of SCI

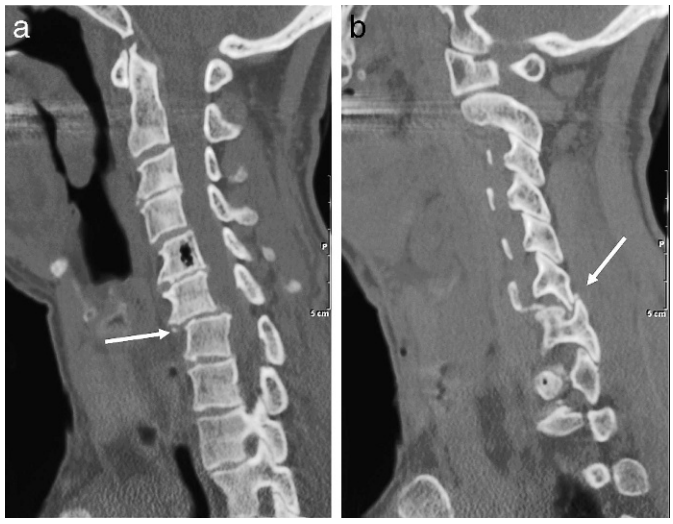

Figure 15. *Hyperflexion injury. (a) Sagittal CT demonstrates anterolisthesis of C6–C7 (arrow). (b) Sagittal CT demonstrates a jumped facet (arrow). The tip of the inferior articular process of C6 is fractured.*

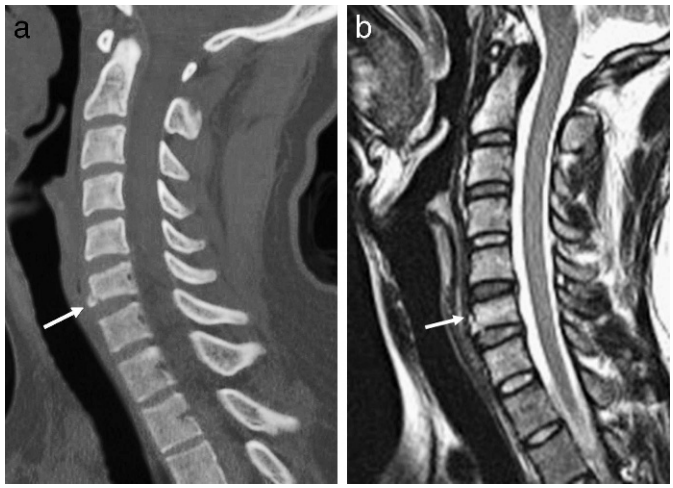

Figure 16. *Flexion-teardrop fracture. (a) Sagittal CT shows mild compression deformity and a small fracture of the anterior-inferior C6 vertebral body (arrow). (b) Sagittal T2-weighted image shows the fracture and an associated anterior longitudinal ligament injury (arrow).*

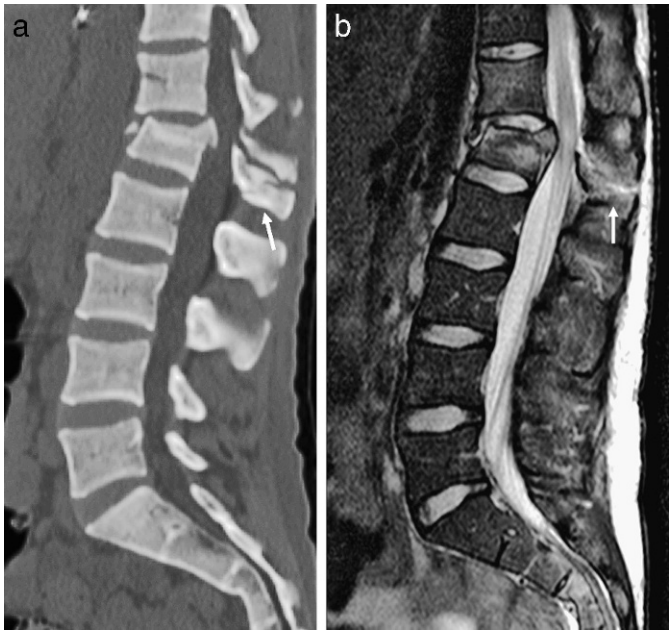

Figure 17. *Chance-type fracture. (a) Sagittal CT demonstrates compression deformity of the L1 vertebral body with distraction of the posterior elements (arrow). (b) Sagittal T2-weighted image demonstrates the compression deformity of the L1 vertebral body, as well as edema within the posterior elements (arrow). Note that the retropulsed fragments compress the conus medullaris with mild associated edema.*

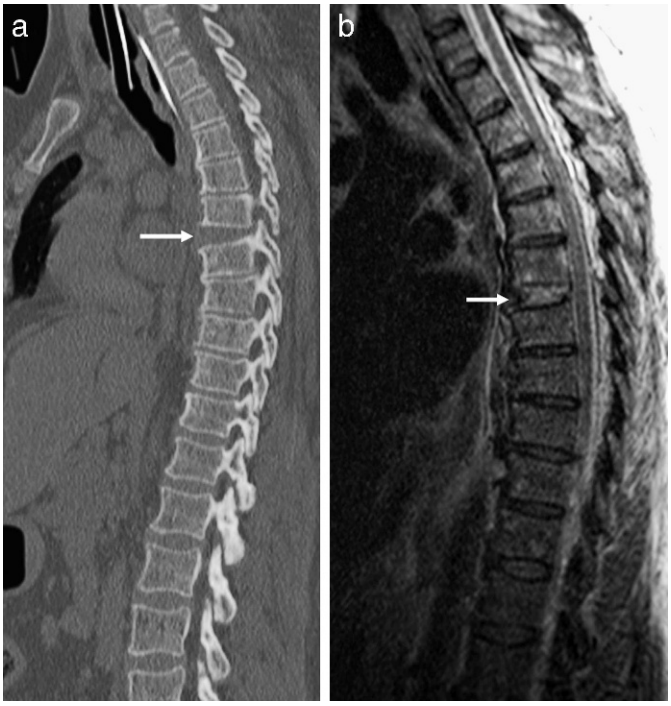

Figure 19. *Hyperextension injury. (a) Sagittal CT demonstrates widening of the anterior T6–T7 disk space (arrow). (b) Sagittal T2-weighted image demonstrates widening of the disk space and edema within the intervertebral disk (arrow).*

include DWI, diffusion tensor imaging, MR spectroscopy, and functional MRI. Although much more widely used in the brain, DWI has on occasion detected SCI that was not seen on conventional sequences (12). Diffusion tensor imaging is an application of DWI that exploits diffusion anisotropy in white matter tracts of the central nervous system to visualize either their normal course or their disruption in the setting of pathology. Recent research has suggested that diffusion tensor imaging can demonstrate more extensive injury to the cord than has heretofore been evident, although to date histologic correlation has been lacking (11).

MR spectroscopy is not routinely used in the assessment of SCI, but one investigation revealed that the concentration of N-acetyl aspartate in the thalamus was negatively correlated with neuropathic pain after SCI (45). An additional recent study demonstrated decreased N-acetyl aspartate within the injured spinal cord and possibly increased lactate, suggesting a role for ischemia in the development of myelopathy (46).

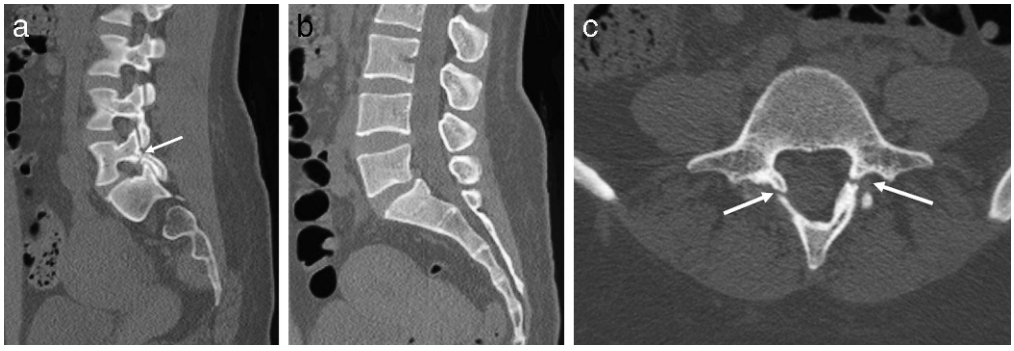

Figure 18. *Spondylolysis. (a) Sagittal CT showing an L5 pars defect (arrow). (b) Sagittal CT showing minimal anterolisthesis of L5 on S1. (c) Axial CT showing bilateral L5 pars defects (arrows).*

Figure 20. *Hyperextension injury. Sagittal T2-weighted image in a different patient shows marked widening and distraction of C2–C3 disk space with cord compression and edema/hemorrhage (arrows).*

Figure 22. *Ligamentous injury. Sagittal T2-weighted image showing injury to the anterior longitudinal ligament (black arrow) and posterior longitudinal ligament (white arrow) with subluxation and cord compression.*

In the realm of functional MRI, cortical activation after nonpainful anorectal stimulation has indicated the presence (in a significant subset of patients) of residual sensory pathways thought to be completely disrupted after injury. This work, if further validated, could result in reclassification of some patients judged to have a neurologically complete deficit. (47).

CONCLUSIONS

Imaging of vertebral and SCI is an essential tool in patient management. CT and MRI are complementary in the assessment of vertebral fractures and vascular abnormalities. MRI is advantageous in the evaluation of ligamentous integrity and is unique in its visualization of internal derangement of the spinal cord, both in acute and chronic settings. Plain radiography has been reduced to a more limited, adjunctive role, and patients can now almost always be spared the discomfort and potential risks of myelography. An understanding of the varying manifestations of SCI has progressed, the significance of which will be enhanced by further advances in therapy, as well as by novel imaging techniques.

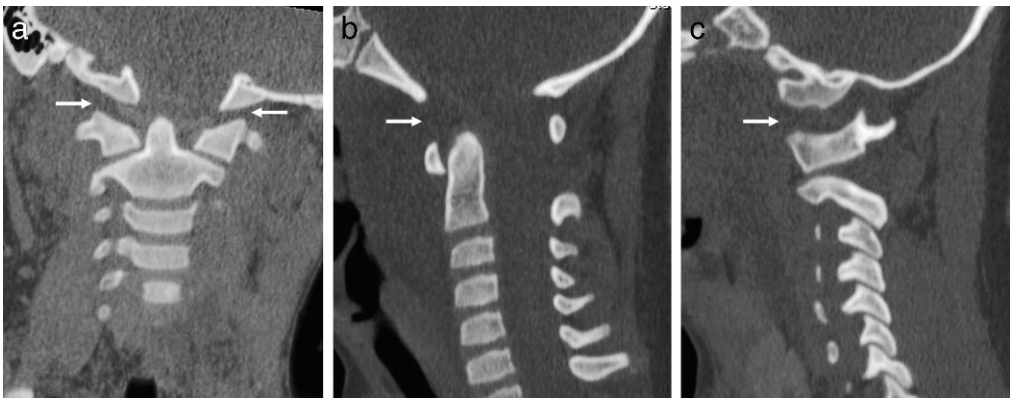

Figure 21. *Atlanto-occipital distraction injury. (a) Coronal CT show marked widening of the atlanto-occipital space in a child (arrow). (b) Sagittal CT shows the widened atlanto-occipital interval (arrow). (c) Parasagittal CT shows the widened atlanto-occipital interval (arrow).*

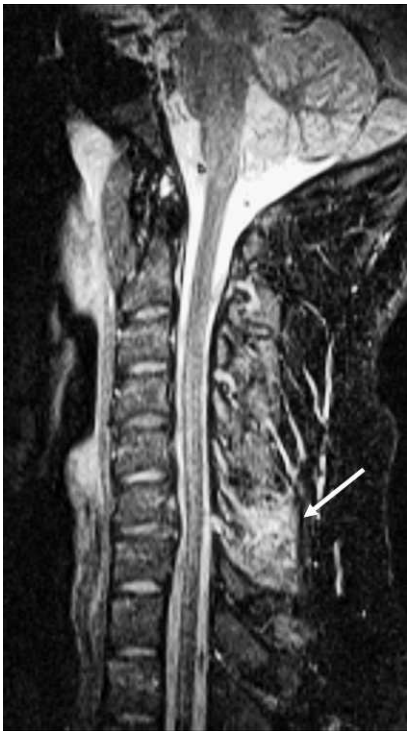

Figure 23. *Ligamentous injury. Sagittal STIR sequence in a different patient demonstrates interspinous ligament injury (arrow).*

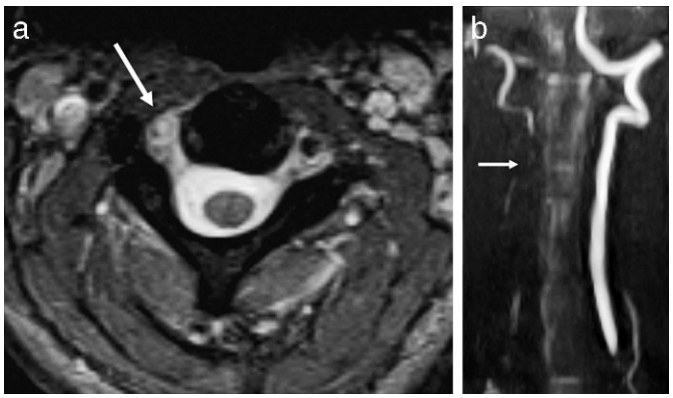

Figure 24. *Vertebral artery injury. (a) Axial T2-weighted image demonstrates loss of the normal flow void within the right vertebral artery consistent with dissection (arrow). Note the normal dark flow void in the left vertebral artery. (b) This was confirmed on a coronal maximum intensity projection view with MR angiography (arrow).*

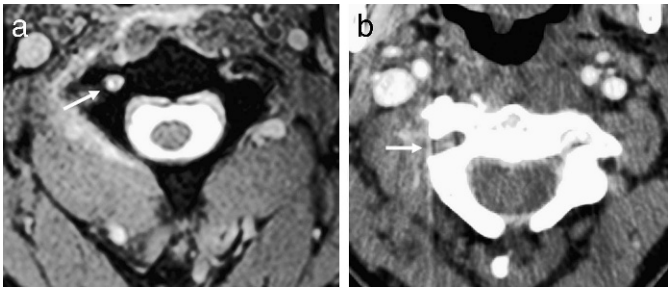

Figure 25. *Vertebral artery injury. (a) Axial T2-weighted image shows loss of the normal flow void within the right vertebral artery (arrow). (b) Lack of right vertebral opacification is also seen on the axial CT angiogram in the same patient (arrow).*

REFERENCES

1. Ross JS, Brant-Zawadzki M, Moore KR, et al. *Diagnostic Imaging: Spine.* 1st ed. Salt Lake City, UT: Amirsys Inc; 2005.
2. Nuñez DB Jr, Quencer RM. The role of helical CT in the assessment of cervical spine injuries. *AJR Am J Roentgenol.* 1998;171(4):951–957.
3. Mann FA, Cohen WA, Linnau KF, Hallam DK, Blackmore CC. Evidence-based approach to using CT in spinal trauma. *Eur J Radiol.* 2003;48(1):39–48.
4. Crim JR, Tripp D. Multidetector CT of the spine. *Semin Ultrasound CT MR.* 2004;25(1):55–66.
5. Griffen MM, Frykberg ER, Kerwin AJ, et al. Radiographic clearance of blunt cervical spine injury: plain radiograph or computed tomography scan? *J Trauma.* 2003;55(2):222–226.
6. Sliker CW. Blunt cerebrovascular injuries: imaging with multidetector CT angiography. *Radiographics.* 2008;28(6):1689–1708; discussion 1709–11710.
7. Eastman AL, Chason DP, Perez CL, McAnulty AL, Minei JP. Computed tomographic angiography for the diagnosis of blunt cervical vascular injury: is it ready for primetime? *J Trauma.* 2006;60(5):925–929.
8. Shapiro MD. MR imaging of the spine at 3T. *Magn Reson Imaging Clin N Am.* 2006;14(1):97–108.
9. Jacobs MA, Ibrahim TS, Ouwerkerk R. AAPM/RSNA physics tutorials for residents: MR imaging: brief overview and emerging applications. *Radiographics.* 2007;27(4):1213–1229.
10. Bitar R, Leung G, Perng R, et al. MR pulse sequences: what every radiologist wants to know but is afraid to ask. *Radiographics.* 2006;26(2):513–537.
11. Shanmuganathan K, Gullapalli RP, Zhuo J, Mirvis SE. Diffusion tensor MR imaging in cervical spine trauma. *AJNR Am J Neuroradiol.* 2008;29(4):655–659.
12. Shen H, Tang Y, Huang L, et al. Applications of diffusion-weighted MRI in thoracic SCI without radiographic abnormality. *Int Orthop.* 2007;31(3):375–383.
13. Kumar R, Lerski RA, Gandy S, Clift BA, Abboud RJ. Safety of orthopedic implants in magnetic resonance imaging: an experimental verification. *J Orthop Res.* 2006;24(9):1799–1802.
14. Shellock FG. Magnetic resonance safety update 2002: implants and devices. *J Magn Reson Imaging.* 2002;16(5):485–496.
15. Shellock FG, Spinazzi A. MRI safety update 2008: part 2, screening patients for MRI. *AJR Am J Roentgenol.* 2008;191(4):1140–1149.
16. Levine GN, Gomes AS, Arai AE, et al. Safety of magnetic resonance imaging in patients with cardiovascular devices: an American Heart Association scientific statement from the Committee on Diagnostic and Interventional Cardiac Catheterization, Council on Clinical Cardiology, and the Council on Cardiovascular Radiology and Intervention: endorsed by the American College of Cardiology Founda-

tion, the North American Society for Cardiac Imaging, and the Society for Cardiovascular Magnetic Resonance. *Circulation.* 2007;116(24):2878–2891.
17. Kanal E, Barkovich AJ, Bell C, et al. ACR guidance document for safe MR practices: 2007. *AJR Am J Roentgenol.* 2007; 188(6):1447–1474.
18. Holmes JF, Mirvis SE, Panacek EA, Hoffman JR, Mower WR, Velmahos GC, for the NEXUS Group. Variability in computed tomography and magnetic resonance imaging in patients with cervical spine injuries. *J Trauma.* 2002; 53(3):524–529; discussion 530.
19. Nogueira-Barbosa MH, Defino HL. Multiplanar reconstructions of helical computed tomography in planning of atlanto-axial transarticular fixation. *Eur Spine J.* 2005;14(5): 493–500.
20. Pretorius ES, Fishman EK. Volume-rendered three-dimensional spiral CT: musculoskeletal applications. *Radiographics.* 1999;19(5):1143–1160.
21. Kasimatis GB, Panagiotopoulos E, Megas P, et al. The adult SCI without radiographic abnormalities syndrome: magnetic resonance imaging and clinical findings in adults with spinal cord injuries having normal radiographs and computed tomography studies. *J Trauma.* 2008;65(1):86–93.
22. Koyanagi I, Iwasaki Y, Hida K, Akino M, Imamura H, Abe H. Acute cervical cord injury without fracture or dislocation of the spinal column. *J Neurosurg.* 2000;93(suppl 1):15–20.
23. Miyanji F, Furlan JC, Aarabi B, Arnold PM, Fehlings MG. Radiology. Acute cervical traumatic spinal cord injury: MR imaging findings correlated with neurologic outcome: prospective study with 100 consecutive patients. *Radiology.* 2007;243(3):820–827.
24. Kulkarni MV, FJ Bondurant FJ, Rose SL, Narayana PA. 1.5 tesla magnetic resonance imaging of acute spinal trauma. *Radiographics.* 1988;8(6):1059–1082.
25. Leypold BG, Flanders AE, Burns AS. The early evolution of spinal cord lesions on MR imaging following traumatic spinal cord injury. *Am J Neuroradiol.* 2008;29(5):1012–1016.
26. Yamashita Y, Takahashi M, Matsuno Y, et al. Chronic injuries of the spinal cord: assessment with MR imaging. *Radiology.* 1990;175(3):849–854.
27. Lee TT, Arias JM, Andrus HL, Quencer RM, Falcone SF, Green BA. Progressive posttraumatic myelomalacic myelopathy: treatment with untethering and expansive duraplasty. *J Neurosurg.* 1997;86(4):624–628.
28. Falcone S, Quencer RM, Green BA, Patchen SJ, Post MJ. Progressive posttraumatic myelomalacic myelopathy: imaging and clinical features. *AJNR Am J Neuroradiol.* 1994; 15(4):747–754.
29. Potter K, Saifuddin A. Pictorial review: MRI of chronic spinal cord injury. *Br J Radiol.* 2003;76(905):347–352.
30. Curati WL, Kingsley DP, Kendall BE, Moseley IF. MRI in chronic spinal cord trauma. *Neuroradiology.* 1992;35(1): 30–35.
31. Rao SK, Wasyliw C, Nunez DB Jr. Spectrum of imaging findings in hyperextension injuries of the neck. *RadioGraphics.* 2005;25(5):1239–1254.
32. Patel RV, DeLong W Jr, Vresilovic EJ. Evaluation and treatment of spinal injuries in the patient with polytrauma. *Clin Orthop Relat Res.* 2004;May(422):43–54.
33. Atlas SW, Regenbogen V, LF Rogers LF, Kim KS. The radiographic characterization of burst fractures of the spine. *AJR Am J Roentgenol.* 1986;147(3):575–582.
34. Kim KS, Chen HH, Russell EJ, Rogers LF. Flexion teardrop fracture of the cervical spine: radiographic characteristics. *AJR Am J Roentgenol.* 1989;152(2):319–326.
35. Bernstein MP, Mirvis SE, Shanmuganathan K. Chance-type fractures of the thoracolumbar spine: imaging analysis in 53 patients. *AJR Am J Roentgenol.* 2006;187(4):859–868.
36. Deliganis AV, Baxter AB, Hanson JA, et al. Radiologic spectrum of craniocervical distraction injuries. *Radiographics.* 2000;20(special issue):S237–S250.
37. Lustrin ES, Karakas SP, Orlando Ortiz AO, et al. Pediatric cervical spine: normal anatomy, variants, and trauma. *Radiographics* 2003;23(3):539–560.
38. DeMarco JK, Huston J III, Nash AK. Extracranial carotid MR imaging at 3T. *Magn Reson Imaging Clin N Am.* 2006;14(1): 109–121.
39. Jewells V, Castillo M. MR angiography of the extracranial circulation. *Magn Reson Imaging Clin N Am.* 2003;11(4): 585–597.
40. Taneichi H, Suda K, Kajino T, Kaneda K. Traumatically induced vertebral artery occlusion associated with cervical spine injuries: prospective study using magnetic resonance angiography. *Spine.* 2005;30(17):1955–1962.
41. Torina PJ, Flanders AE, Carrino JA, et al. Incidence of vertebral artery thrombosis in cervical spine trauma: correlation with severity of spinal cord injury. *AJNR Am J Neuroradiol.* 2005;26(10):2645–2651.
42. Friedman D, Flanders A, Thomas C, Millar W. Vertebral artery injury after acute cervical spine trauma: rate of occurrence as detected by MR angiography and assessment of clinical consequences. *AJR Am J Roentgenol.* 1995; 164(2):443–447.
43. Vertinsky AT, Schwartz NE, Fischbein NJ, Rosenberg J, Albers GW, Zaharchuk G. Comparison of multidetector CT angiography and MR imaging of cervical artery dissection. *AJNR Am J Neuroradiol.* 2008;29(9):1753–1760.
44. Lum C, Chakraborty S, Schlossmacher M, et al. Vertebral artery dissection with a normal-appearing lumen at multisection CT angiography: the importance of identifying wall hematoma. *AJNR Am J Neuroradiol.* 2009;30(4):787–792.
45. Pattany PM, Yezierski RP, Widerström-Noga EG, et al. Proton magnetic resonance spectroscopy of the thalamus in patients with chronic neuropathic pain after spinal cord injury. *AJNR Am J Neuroradiol.* 200;23(6):901–905.
46. Holly LT, Freitas B, McArthur DL, Salamon N. Proton magnetic resonance spectroscopy to evaluate spinal cord axonal injury in cervical spondylotic myelopathy. *J Neurosurg Spine.* 2009;10(3):194–200.
47. Wietek BM, Baron CH, Erb M, et al. Cortical processing of residual ano-rectal sensation in patients with spinal cord injury: an fMRI study. *Neurogastroenterol Motil.* 2008;20(5): 488–497.